

Supplementary Materials

Mountain jade: A new high-elevation microendemic species of the genus *Zhangixalus* (Amphibia: Anura: Rhacophoridae) from Laos

Peter Brakels^{1,#}, Tan Van Nguyen^{2,3,#}, Parinya Pawangkhanant⁴, Sabira S. Idiiatullina⁵, Sengvilay Lorphengsy⁶, Chatmongkon Suwannapoom^{4,*}, Nikolay A. Poyarkov^{5,7,*}

¹IUCN Laos PDR, Vientiane 01160, Lao PDR

²Institute for Research and Training in Medicine, Biology and Pharmacy, Duy Tan University, Da Nang 550000, Vietnam

³Faculty of Medicine, Duy Tan University, Da Nang 550000, Vietnam

⁴Division of Fishery, School of Agriculture and Natural Resources, University of Phayao, Phayao, Thailand

⁵Department of Vertebrate Zoology, Biological Faculty, Lomonosov Moscow State University, Moscow 119234, Russia

⁶Biotechnology and Ecology Institute, Ministry of Science and Technology, Vientiane 01000, Lao PDR

⁷Joint Russian-Vietnamese Tropical Research and Technological Center, Nghia Do, Cau Giay, Hanoi, Vietnam

#Authors contributed equally to this work

*Corresponding authors, E-mail: chatmongkonup@gmail.com; n.poyarkov@gmail.com

SUPPLEMENTARY MATERIALS AND METHODS

Specimen collection and preservation. Field surveys were conducted in July 2020 in Phou Samsoum Mountain (PSM) in Xiengkhouang Province, northeast Laos (Figure 1A). Geographic coordinates and elevation were obtained using a Garmin GPSMAP 64CSx (USA) and recorded in WGS84 datum. Specimens were euthanized with 20% benzocaine and femoral muscles were collected for genetic analysis and stored in 90% ethanol prior to specimen preservation. Specimens were subsequently preserved in 70% ethanol and deposited in the herpetological collections of the Biotechnology and Ecology Institute Ministry of Science and Technology of Laos (BEI, Veintiane, Laos), the School of Agriculture and Natural Resources, University of Phayao (AUP, Phayao, Thailand) and the Zoological Museum of Lomonosov Moscow State University (ZMMU, Moscow, Russia).

Laboratory methods. For molecular phylogenetic analyses, we extracted total genomic DNA from ethanol-preserved femoral muscle tissue using standard phenol-chloroform-proteinase K extraction procedures with consequent isopropanol precipitation; to a final concentration of ~1 mg/mL (protocols followed Hillis et al., 1996 and Sambrook & Russell, 2001). We visualized the isolated total genomic DNA in agarose electrophoresis in the presence of ethidium bromide. We measured the concentration of total DNA in 1 μ L using a NanoDrop 2000 (Thermo Scientific, USA), and consequently adjusted the concentration to ca. 100 ng DNA/ μ L.

We amplified mtDNA fragments covering partial sequences of the 16S rRNA mtDNA gene to obtain a 1918 bp length continuous fragment of mtDNA. We also amplified 655 bp of the 5'-end of the first subunit of cytochrome c oxidase mtDNA gene (*COI*). The 16S rRNA gene is widely applied in biodiversity surveys in amphibians (Vences et al., 2005a, 2005b; Vieites et al., 2009), and has been used in most recent phylogenetic studies on Rhacophoridae (Jiang et al., 2019; Li et al., 2008, 2012; Nguyen et al., 2020; Ninh et al., 2020; Pan et al., 2017; Poyarkov et al., 2018). The *COI* gene is widely known as a barcoding marker for amphibians as well as other vertebrates (Murphy et al., 2013). We performed DNA amplification in 20 μ L reactions using ca. 50 ng genomic DNA, 10 nmol of each primer, 15 nMol of each dNTP, 50 nMol additional MgCl₂, Taq PCR buffer (10 mmol/L Tris-HCl, pH 8.3, 50 mmol/L KCl, 1.1 mmol/L MgCl₂, and 0.01% gelatin), and 1 unit of Taq DNA polymerase. Primers used in PCR and sequencing of were obtained from previous studies (for 16S rRNA gene: Hedges, 1994; Li et al., 2008; Poyarkov et al., 2018; for *COI* gene: Che et al., 2012). The PCR conditions included an initial denaturation step of 5 min at 94 °C and 43 cycles of denaturation for 1 min at 94 °C, primer annealing for 1 min with the TouchDown program from 65 °C to 55 °C reducing 1 °C every cycle, extension for 1 min at 72 °C, and final extension step for 5 min at 72 °C.

The PCR products were loaded onto 1.5% agarose gels in the presence of ethidium bromide and visualized via agarose electrophoresis. When distinct bands were produced, we purified the PCR products using 2 μ L of a 1:4 dilution of ExoSapIt (Amersham, USA) per 5 μ L of PCR product

prior to cycle sequencing. The 10 μ L sequencing reaction included 2 μ L of template, 2.5 μ L of sequencing buffer, 0.8 μ L of 10 pmol primer, 0.4 μ L of BigDye Terminator v3.1 Sequencing Standard (Applied Biosystems, USA), and 4.2 μ L of water. The cycle sequencing used 35 cycles of 10 s at 96 °C, 10 s at 50 °C, and 4 min at 60 °C. We purified the cycle sequencing products by ethanol precipitation. We carried out sequence data collection and visualization on an ABI 3730xl Automated Sequencer (Applied Biosystems, USA). The obtained sequences were deposited in GenBank under accession numbers OQ288104-OQ288107, OQ297601, OQ305233-OQ305236 (see Supplementary Table S1).

Phylogenetic analyses. To reconstruct the matrilineal genealogy, we used 16S rRNA and *COI* sequences of the *Zhangixalus* sp. from Xiengkhouang Province of Laos, as well as the homologous sequences of 38 out of 40 currently recognized *Zhangixalus* species obtained from the earlier phylogenetic studies of the genus (e.g., Mathipi et al., 2021; Nguyen et al., 2020; Ninh et al., 2020; Pan et al., 2017; Yu et al., 2019; see Supplementary Table S1). GenBank accession numbers, museum vouchers, and localities of origin for sequences used in this study are summarized in Supplementary Table S1. We also added the homologous sequences of *Leptomantis gauni* and *Rhacophorus kio*, representing the sister taxa of *Zhangixalus*; the sequence of *Polypedates leucomystax* was used as an outgroup (Jiang et al., 2019). In total, we obtained 16S rRNA and *COI* sequence data from 45 specimens, including four specimens of *Zhangixalus* sp. from Xiengkhouang, 38 sequences of all other species of *Zhangixalus*, three outgroup sequences of other Rhacophoridae representatives (*Leptomantis*, *Rhacophorus*, and *Polypedates*) (see Supplementary Table S1).

We initially aligned nucleotide sequences using ClustalX 1.81 (Thompson et al., 1997) with default parameters, and then optimized them manually in BioEdit 7.0.5.2 (Hall, 1999). We used MODELTEST v.3.06 (Posada & Crandall, 1998) to estimate the optimal evolutionary models to be used for dataset analysis. The best-fitting model for the 16S rRNA gene fragment was the GTR+I+G model of DNA evolution, as suggested by the Akaike Information Criterion (AIC). The best-fitting models selected for the *COI* dataset were SYM+I for the first, F81+I for the second, and HKY+G for the third codon positions, as suggested by the Akaike Information Criterion (AIC). We determined mean uncorrected genetic distances (*p*-distances) between sequences with MEGA 6.0 (Tamura et al., 2013).

We inferred matrilineal genealogy using Bayesian inference (BI) and maximum-likelihood (ML) approaches. We conducted BI in MrBayes 3.1.2 (Ronquist & Huelsenbeck, 2003); Metropolis-coupled Markov chain Monte Carlo (MCMCMC) analyses were run with one cold chain and three heated chains for one million generations, with sampling every 100 generations. We performed five independent MCMCMC runs and the initial 2 500 trees were discarded as burn-in. We assessed confidence in tree topology by the frequency of nodal resolution (posterior probability; BI PP) (Huelsenbeck et al., 2001). We *a priori* considered BI PP 0.95 or greater as significant support (Leaché & Reeder, 2002).

We conducted the ML analysis in the IQ-TREE webserver (<http://iqtree.cibiv.univie.ac.at/>). We employed 1,000 bootstrap pseudoreplicates via the ultrafast bootstrap (UFBS; Hoang et al., 2018) approximation algorithm, and nodes having ML UFBS values of 95 and above were a-priori considered highly supported, while the nodes with values of 90–94 were considered well-supported, and the nodes with values of 70–89 were considered as tendencies. Lower values were considered to indicate no support.

Morphological description. Measurements were taken to the nearest 0.1 mm with a Mitutoyo digital caliper. The descriptions of the morphological characteristics of adults and larvae followed Poyarkov et al. (2018) and Poyarkov et al. (2015), respectively. Sex was determined by direct observation of calling and by examination of the nuptial pads and vocal sac in males. Comparative data on morphological and bioacoustic characteristics of other *Zhangixalus* species were obtained from previous publications.

The morphometrics of adults and character terminology followed Poyarkov et al. (2018): SVL (snout-vent length); A-G (axilla to groin, distance from posterior base of forelimb at its emergence from body to anterior base of hind limb at its emergence from body); HW (head width at greatest cranial width); HL (head length from rear of lower jaw to tip of the snout); HD (head depth, greatest transverse depth of head, taken beyond interorbital region); UEW (upper eyelid width, greatest width of upper eyelids); IOD (interorbital distance); ED (horizontal diameter of eye); TD (horizontal diameter of tympanum); ESL (tip of snout-eye distance); IND (internarial distance between nostrils); END (eye to nostril distance from anterior corner of eye to nostril); TED (tympanum-eye distance from anterior edge of tympanum to posterior corner of eye); NS (distance from nostril to tip of snout); FLL (length of forelimb from tip of disk of finger III to axilla); HML (humerus length from axilla to elbow); LAL (forearm length, from elbow to base of outer palmar tubercle); ML (hand length from tip of third digit to base of outer palmar tubercle); 1FLi (first finger length, from base of inner palmar tubercle to tip finger); 1FLo (first finger length in inner); 2FLi (second finger length in inner); 3FLi (third finger length in inner); 4FLi (fourth finger length in inner); FTD (maximal diameter of disk of finger III); NPL (nuptial pad length, measured for males only); MCTe (length of external metacarpal tubercle); HLL (length of hindlimb from tip of disk of toe IV to groin); FL (femur length); TL (tibia length); TTL (tibiotarsus length from the posterior edge of tibia to the anterior edge of inner metatarsal tubercle); FOT (foot length from tip of fourth toe to the anterior edge of the inner metatarsal tubercle); 1TLi (first toe length, from the base of inner carpal tubercle to the tip); 1TLo (first toe length in outer); 2TLi (second toe length in inner); 3TLi (third toe length in inner); 4TLi (fourth toe length in inner); 5TLi (fifth toe length in inner); HTD (diameter of fourth toe tip, greatest diameter of disk on fourth toe); MTTi (length of internal metatarsal tubercle); IMW (inner metatarsal tubercle width). Additional measurements of the holotype of *Zhangixalus nigropunctatus* (Liu, Hu & Yang) [CIB 590405] followed Li et al. (2011) and included the following characters: FLL-2 (forelimb length excluding the length of the humerus, measured from elbow to tip of third finger); and FTL (length of tarsus and foot from the

posterior edge of tibia to the end of the fourth toe). Subarticular tubercle and webbing formulas follow Savage (1975). All measurements were taken on the right side of the examined specimen. Sex was determined by gonadal inspection following dissection.

Morphological description of larval stages included the following Poyarkov et al. (2015): TL (total length); BL (body length); TaL (tail length); BW (maximal body width); BH (maximal body height); TH (maximal tail height); SVL (snout-vent length); SSp (snout-spiracle length); UF (maximal upper tail fin height); LF (maximal lower fin height); IN (internarial distance); IP (interpupilar distance); RN (rostronarial distance); NP (narrow-pupilar distance); ED (eye diameter); ODW (oral disk width). LTRF (labial tooth row formula) was recorded following Wassersug et al. (1981). Tadpoles were staged after Gosner (1960); morphometrics followed Grosjean (2001).

Comparative data on the morphology and taxonomy of *Zhangixalus* were obtained from previous publications on the genus (Chen et al., 2018; Chou et al., 2007; Fei et al., 2010; Jiang et al., 2016, 2019; Li et al., 2012; Liu et al., 2017, 2020; Mo et al., 2016; Nguyen et al., 2020; Ninh et al., 2020; Ohler & Deuti, 2018; Ohler et al., 2000; Orlov et al., 2001; Pan et al., 2017; Rao et al., 2006; Yu et al., 2019; Zhang et al., 2011). Comparative data on the morphology of *Zhangixalus nigropunctatus* (Liu, Hu & Yang) tadpoles were obtained from Editorial Committee of Zoology of China, Chinese Academy of Sciences (2009) and Fei et al. (2010).

Bioacoustic analysis. Advertisement calls of the newly discovered *Zhangixalus* population were recorded in situ at the breeding site (coordinates N 19.131 °, E 103.784 °; elevation 2066 m asl.) on 15 July 2020 at 2030 h and at 16.5 °C using a portable digital audio recorder Zoom h5 (ZOOM Corporation, Tokyo, Japan) in stereo mode with 48 kHz sampling frequency and 16-bit precision. The temperature was measured at the calling site immediately after the audio recording with a digital thermometer KTJ TA218A Digital LCD Thermometer-Hydrometer. Calls were analyzed using Avisoft SASLab Pro software v.5.2.05 (Avisoft Bioacoustics, Germany); the analyses generally followed Poyarkov et al. (2018).

In total, six advertisement calls from two individuals (holotype AUP02505 and paratype ZMMU A-7781) were recorded. The total duration of the recordings was 541.86 s. Calls were analyzed using Avisoft SASLab Pro software v. 5.2.05; spectrograms for analysis were created using Hamming window, FFT-length 1024 points, frame 100%, and overlap 93.75%. Figure spectrograms were created using Hamming window, FFT-length 512 points, frame 50%, and overlap 93.75%. We measured the duration of each note (s) number of pulses per note, pulse duration (measured separately for the first, the second and the third pulses, s), internote interval (s), note repetition rate (notes per second), and the dominant frequency (= frequency of maximum amplitude, Hz). Notes (or pulses) per second were calculated by counting the number of notes (or pulses) within each call, minus one, and dividing that number by the call duration (or duration of the note). All numeral parameters are given as mean \pm SE, the minimum and maximum values are given in parentheses (min–max).

Comparative advertisement call characteristics for *Zhangixalus* species were taken from

references, with advertisement calls known only for five of the 40 known species of *Zhangixalus* (Fang et al., 2019; Matsui & Wu, 1994; Nguyen et al., 2020; Wang et al., 2012).

SUPPLEMENTARY RESULTS

Measurements of the holotype and additional morphological information on *Zhangixalus nigropunctatus* (Liu, Hu & Yang). The following measurements of the holotype of *Zhangixalus nigropunctatus* (Liu, Hu & Yang) [CIB 590405] were taken by one of us (NAP), additional measurements of this specimen were obtained from the paper by Li et al. (2011). For abbreviations of the additional measurements see Supplementary materials and methods. Measurements of CIB 590405 (all in mm): SVL: 36.5; A-G: 20.0; HW: 12.5; HL: 12.2; HD: 5.1; UEW: 3.0; IOD: 4.0; ED: 4.5; TD: 1.5; ESL: 5.1; IND: 3.4; END: 2.6; TED: 1.5; NS: 2.5; FLL: 26.0; HML: 7.0; LAL: 8.0; ML: 10.2; FLL-2: 18.2; FTD: 1.8; HLL: 48.0; FL: 12.0; TL: 14.0; TTL: 8.0; FOT: 14.8; FTL: 22.8; HTD: 1.8.

Photograph of a male *Zhangixalus nigropunctatus* (Liu, Hu & Yang) from Yushe National Forest Park (N 26.46 °, E 104.81 °; elevation 2070 m a.s.l.), Guizhou Province, China, kindly provided by Jian Wang (SYS, China) is presented in Supplementary Figure S5.

Larval morphology description. Tadpoles in the developmental stage 35 of Gosner (1960) were assigned to the new species based on 16S partial sequences obtained for one specimen ZMMU A-7783. Measurements of tadpoles of the new species are presented in Supplementary Table S4;

General appearance of the tadpoles in preservative: The tadpoles are medium-sized (TL = 25.1–39.8 mm), lentic: benthic (Altig & McDiarmid, 1999), and are classified as generalized exotrophic tadpoles of Orton's (Orton, 1953) type IV lacking obvious specializations. Dorsal coloration is uniform light-brown from the snout to the tip of the tail including fins (Supplementary Figure S4A). Dark-brown marbled pattern is present on dorsal tail fin and on the dorsal surfaces of body. Dorsal and dorsolateral pigmentation of the body is same dense as the tail pigmentation. The tail musculature coloration varies from light brown to ochre (see Supplementary Figure S4A). The ventral and ventrolateral body sides are white to yellow and more or less pigmented. Belly is translucent and the intestine is visible through the body.

The following description is based on a single tadpole ZMMU A-7783-1 with SVL 39.8 mm. In dorsal view, body elliptical with a slightly pointed snout (Supplementary Figure S4A) with its widest portion being at midbody (body width 0.56 times of body length). Eyes of moderate size (eye diameter 0.11 times of body length), with dorsolateral orientation, directed more laterally than anteriorly, slightly bulging, not visible in ventral view. Nares small, rounded, not rimmed, positioned dorsolaterally in slightly anterolateral direction. Naris notably closer to snout than to pupil (rostronarial distance 0.36 times of naropupilar distance). Internarial distance about 0.44 times of interpupilar distance. Nasolacrimal duct from the naris to the anterior corner of the eye not discernable.

In lateral view, body slightly depressed (body height 0.86 times of body width), snout slightly

rounded. Spiracle sinistral, positioned at midbody with ventrolateral orientation (distance from snout tip to opening of spiracle 0.59 times of body length), conical, with posterodorsal orientation and entirely attached to the body. Spiracle opening oval; vent tube partially reduced. Myotomes of the tail musculature well-developed; with parallel orientation in the anterior part of the tail, then gradually tapering, reaching the tip of the tail. Tail fin moderate, tapering at the end. Highest point of the upper fin at the middle of the tail length (maximum height of upper tail fin 0.30 times of maximum tail height). Lower fin slightly smaller than dorsal fin (maximum height of lower tail fin 0.78 times of maximum tail height). Lateral line organs well developed on body and along the the caudal musculature.

Oral disk anteroventrally positioned comprising about 0.34 times of body width, ovoid in shape in relaxed state (see Supplementary Figure S4B), laterally emarginated. Oral disk framed by finger shaped papillae of moderate size except for a large medial gap of the upper labium is slightly narrower than the first keratodont row. Submarginal papillae on the upper labium not discernable; posterior border of the lower labium emarginated with an additional row of submarginal papillae of the same length as the lowest keratodont row. Keratodont row A1 continuous, A2 – A3 divided, A4 – A6 entirely separated by the upper jaw sheath. Keratodont row P1 divided; keratodont rows P2 – P3 of the lower labium undivided. Keratodont row formula (KRF): 1:5+5/1+1:2. Jaw sheaths black, notably serrated (see Supplementary Figure S4B); with upper jaw sheath narrow, stretched into a wide arch; lower jaw sheath V-shaped.

Morphological comparisons. The green dorsum, the white belly, flanks, axilla, ventral surface of forearms, inguinal, anterior and posterior surfaces of thighs covered with irregular black pattern; and the reddish-orange iris distinguishes the new species from 25 nominal *Zhangixalus* species distributed in Indochina, China, India and Myanmar (comparisons detailed in Supplementary Tables S5–S7).

Morphological comparisons of the new species with its sister species *Z. nigropunctatus* appear to be the most pertinent (see Supplementary Figure S5 for life photo of *Z. nigropunctatus*; also see Supplementary Results for measurements of the holotype of this species [CIB 590405]). The new species can be readily distinguished from *Z. nigropunctatus* by coloration in life, in particular by the presence of large irregular black blotches on axilla, flanks, anterior and posterior surfaces of thighs forming continuous pattern (vs. small separated indistinct black spots), by having small back spots on the ventral surfaces of thighs and tarsus (vs. yellowish lacking back spots), and by having bright reddish-orange iris (vs. yellowish-gold). In morphometrics males of the new species can be easily differentiated from *Z. nigropunctatus* by comparatively larger head (HL/SVL 36.7% [N=4] vs. 34.5% [N=20, data from Editorial Committee of Zoology of China, Chinese Academy of Sciences, 2009] in *Z. nigropunctatus*, 33.4% in the holotype of *Z. nigropunctatus*, see Supplementary Results); by having a larger tympanum (TD/SVL 5.9% [N=4] vs. 4.9% [N=20, data from Editorial Committee of Zoology of China, Chinese Academy of Sciences, 2009] in *Z. nigropunctatus*, 4.1% in the holotype of *Z. nigropunctatus*); by having comparatively larger eyes

(ED/SVL 16.7% [N=4] vs. 14.0% in the holotype of *Z. nigropunctatus*); by having larger internarial distance (IND/SVL 12.2% [N=4] vs. 9.3% in the holotype of *Z. nigropunctatus*); and by having comparatively longer hindlimbs (HLL/SVL 141.7% [N=4] vs. 131.5% in the holotype of *Z. nigropunctatus*). Furthermore, the new species is clearly different from *Z. nigropunctatus* in keratodont row formula (KRF) of tadpole mouth discs (1:5+5/1+1:2 vs. 1:3+3/1+1:1 in *Z. nigropunctatus*, data from Editorial Committee of Zoology of China, Chinese Academy of Sciences, 2009). Moreover, the closest known population of *Z. nigropunctatus* in Guizhou Province of China is separated from the range of *Zhangixalus melanoleucus* **sp. nov.** by over 800 km distance, which provides further support for our hypothesis that the differentiation between these taxa reaches the species level. Comparisons of *Zhangixalus melanoleucus* **sp. nov.** with other congeners are detailed in Supplementary Data and summarized in Supplementary Table S5.

Zhangixalus melanoleucus **sp. nov.** can be distinguished from other members of *Z. chenfui* species group by the following combination of morphological characters. The new species differs from *Z. chenfui* (Liu) by having whitish belly without spots (vs. cream with small pale yellow spots), by the presence of irregular black pattern on white flanks, anterior and posterior surfaces of thighs (vs. absence); from *Z. pinglongensis* by having flanks and anterior and posterior surfaces of thighs white with irregular black pattern (vs. black with small white spots), by having ventral surfaces of feet and webbing cream (vs. tangerine), and by reddish-orange iris (vs. silver); from *Z. yaoshanensis* (Liu & Hu) by having flanks, anterior and posterior surfaces of thighs white with irregular black pattern (vs. orange-red without spots), and by having reddish orange iris (vs. grayish-gold); from *Z. jodiae* by having flanks and anterior and posterior surfaces of thighs white with irregular black pattern (vs. axilla cream with large black blotches, groin and front-rear parts of the thigh, ventral surface of tibia black with orange blotches), and by reddish-orange iris (vs. silver).

From other *Zhangixalus* species which have immaculate green dorsum, *Zhangixalus melanoleucus* **sp. nov.** can be further distinguished as follows: from *Z. dorsovireidis* by the presence of nuptial pads (vs. absence), by flanks, anterior and posterior surfaces of thighs white with irregular large black pattern (vs. white to orange with variable small black spots); from *Z. feae* by smaller body size (34.4–36.3 mm in males, 53.7 mm in female vs. 86–111 mm in males, 68–116 mm in females), by having white or grey throat (vs. pale green), by the presence of irregular black pattern on white flanks, anterior and posterior surfaces of thighs (vs. absence), by reddish-orange iris (vs. greenish-gold), by finger webbing reduced (vs. complete); from *Z. leucofasciatus* (Liu & Hu) by having smaller body size in males (34.4–36.3 mm vs. 47.5–49.4 mm), by the presence of an irregular black pattern on flanks, anterior and posterior surfaces of thighs (vs. absence), by reddish-orange iris (vs. yellowish-brown); from *Z. lishuiensis* (Liu, Wang & Jiang) by having the entire belly whitish (vs. anteriorly white, posteriorly yellow), by the presence of an irregular black pattern on flanks, anterior and posterior surfaces of thighs (vs. absence), by reddish-orange iris (vs. yellowish-gold); from *Z. minimus* (Rao, Wilkinson & Liu) by having immaculate white ventral surfaces (vs. spots on belly), by the presence of an irregular black pattern on flanks, anterior and

posterior surfaces of thighs (vs. absence), by reddish-orange iris (vs. yellowish-gold); from *Z. pachyproctus* by having smaller body size (34.4–36.3 mm in males, 53.7 mm in female vs. 73.4–78.2 mm in males, 102.4 mm in female), by the presence of an irregular black pattern on flanks, anterior and posterior surfaces of thighs (vs. absence), by reddish-orange iris (vs. yellowish-gold), and by reduced finger webbing (vs. complete); from *Z. smaragdinus* (Blyth) by having smaller body size (34.4–36.3 mm in males, 53.7 mm in female vs. 57–84 mm in males, 85–112 mm in females), by the presence of an irregular black pattern on flanks, anterior and posterior surfaces of thighs (vs. absence), by reddish-orange iris (vs. yellowish-gold), and by reduced finger webbing (vs. complete); from *Z. zhokaiyae* (Pan, Zhang & Zhang) by having ventral surface whitish (vs. yellowish), by the presence of an irregular black pattern on flanks, anterior and posterior surfaces of thighs (vs. small brown spots), and by reddish-orange iris (vs. yellowish-gold).

Zhangixalus melanoleucus **sp. nov.** further differs from all other congeners by having immaculate green dorsum (vs. green to dark green with small pale yellow to brown dots in *Z. burmanus* (Andersson); green with small brown spots in *Z. dennysi* (Blanford); greenish with red-brown spots in *Z. duboisi* (Ohler, Marquis, Swan & Grosjean); green with round golden spots in *Z. dugritei* (Boulenger); green with dark brown spots in *Z. franki* Ninh, Nguyen, Orlov, Nguyen & Ziegler; green with yellowish-brown spots edged with dark brown in *Z. hongchibaensis* (Li, Liu, Chen, Wu, Murphy, Zhao, Wang & Zhang); green with brown spots in *Z. hui* (Liu); green with small white spots in *Z. hungfuensis* (Liu & Hu); green with brown pattern in *Z. omeimontis* (Stejneger); greenish-yellow with small white or brown spots in *Z. prominanus* (Smith); green with brownish-red spots in *Z. puerensis* (He); numerous light-brown spots with dark yellowish brown edges in *Z. wui* (Li, Liu, Chen, Wu, Murphy, Zhao, Wang & Zhang); and green with few fine white spots in *Z. yinggelingsis* (Chou, Lau & Chan).

Discussion on synonymy of particular *Zhangixalus* species. Our data confirms the synonymy of *Rhacophorus taronensis* Smith and *R. gongshanensis* Yang & Su with *Z. burmanus* (Andersson) as proposed earlier by Ohler (2009); and of *Polypedates pingbianensis* Kou, Hu & Gao with *Z. duboisi* (Ohler, Marquis, Swan & Grosjean) as proposed by Orlov et al. (2002).

REFERENCES

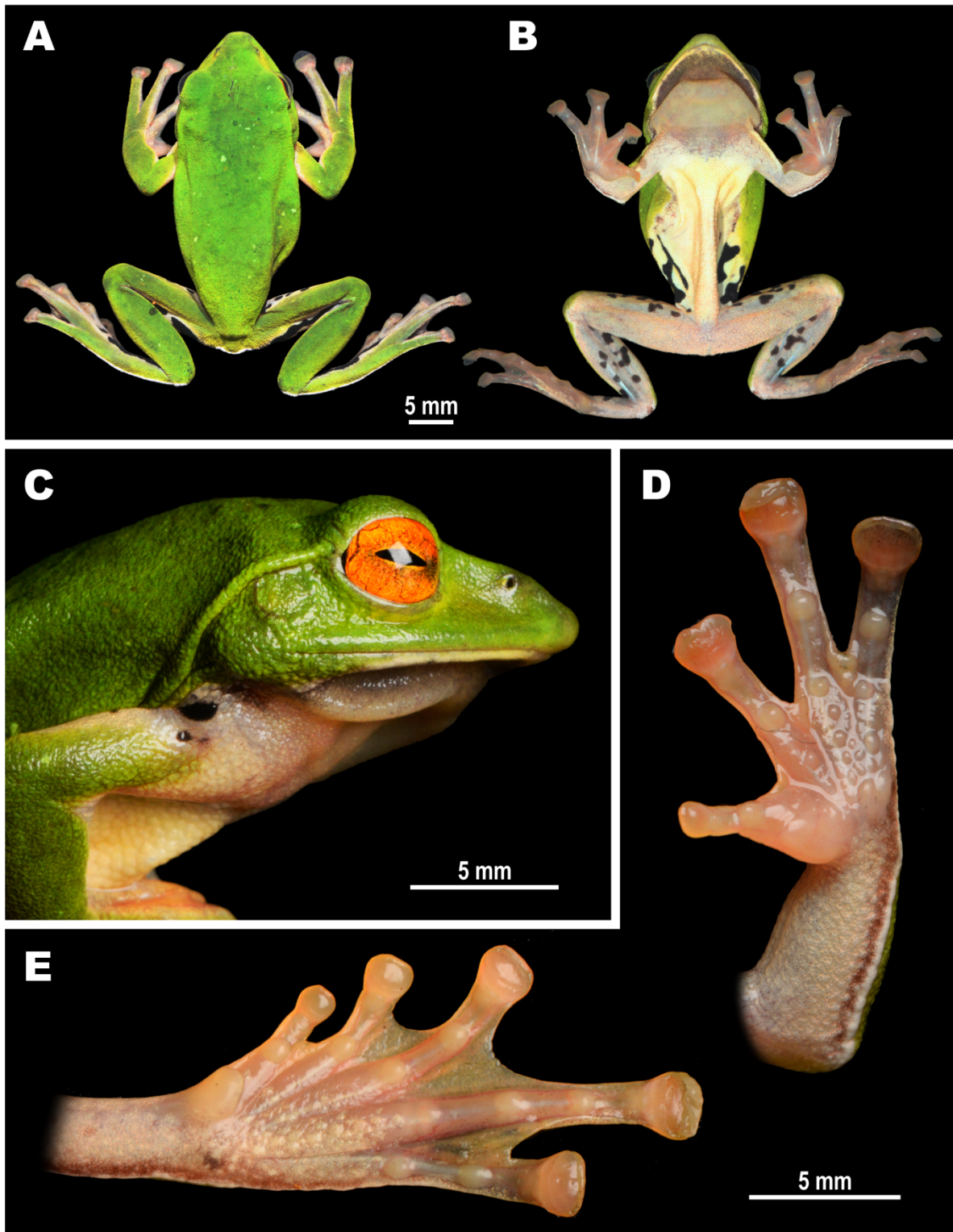
- Altig R, McDiarmid RW. 1999. Body plan: development and morphology. *In*: McDiarmid RW, Altig R. Tadpoles: The Biology of Anuran Larvae. Chicago, London: The University of Chicago Press, 24–51.
- Che J, Chen HM, Yang JX, et al. 2012. Universal COI primers for DNA barcoding amphibians. *Molecular Ecology Resources*, **12**(2): 247–258.
- Chen WC, Liao XW, Zhou SC, et al. 2018. Rediscovery of *Rhacophorus yaoshanensis* and *Theloderma kwangsiensis* at their type localities after five decades. *Zootaxa*, **4379**(4): 484–496.
- Chou WH, Lau MWN, Chan BPL. 2007. A new treefrog of the genus *Rhacophorus* (Anura:

- Rhacophoridae) from Hainan Island, China. *The Raffles Bulletin of Zoology*, **55**(1): 157–165.
- Editorial Committee of Zoology of China, Chinese Academy of Sciences. 2009. *Fauna Sinica: Volume 2: Amphibia Anura*. Beijing: Science Press. (in Chinese)
- Fang K, Zhang BW, Brauth SE, et al. 2019. The first call note of the Anhui tree frog (*Rhacophorus zhoukaiya*) is acoustically suited for enabling individual recognition. *Bioacoustics*, **28**(2): 155–176.
- Fei L, Ye CY, Jiang JP. 2010. *Colored Atlas of Chinese Amphibians*. Chengdu: Sichuan Publishing House of Science and Technology. (in Chinese)
- Gosner KL. 1960. A simplified table for staging anuran embryos and larvae with notes on identification. *Herpetologica*, **16**(3): 183–190.
- Grosjean S. 2001. The tadpole of *Leptobrachium (Vibrissaphora) echinatum* (Amphibia, Anura, Megophryidae). *Zoosystema*, **23**(1): 143–156.
- Hall TA. 1999. BioEdit: a user-friendly biological sequence alignment editor and analysis program for Windows 95/98/NT. *Nucleic Acids Symposium Series*, **41**(2): 95–98.
- Hedges SB. 1994. Molecular evidence for the origin of birds. *Proceedings of the National Academy of Sciences of the United States of America*, **91**(7): 2621–2624.
- Hillis DM, Moritz C, Mable BK. 1996. *Molecular Systematics*. 2nd ed. Sunderland: Sinauer Associates.
- Hoang DT, Chernomor O, von Haeseler A, et al. 2018. UFBoot2: improving the ultrafast bootstrap approximation. *Molecular Biology and Evolution*, **35**(2): 518–522.
- Huang MY, Lv T, Duan RY, et al. 2016. The complete mitochondrial genome of *Rhacophorus dennysi* (Anura: Rhacophoridae) and phylogenetic analysis. *Mitochondrial DNA Part A*, **27**(5): 3719–3720.
- Huelsenbeck JP, Ronquist F, Nielsen R, et al. 2001. Bayesian Inference of phylogeny and its impact on evolutionary biology. *Science*, **294**(5550): 2310–2314.
- Jiang DC, Jiang K, Ren JL, et al. 2019. Resurrection of the genus *Leptomantis*, with description of a new genus to the family Rhacophoridae (Amphibia: Anura). *Asian Herpetological Research*, **10**(1): 1–12.
- Jiang K, Wang K, Yang JX, et al. 2016. Two new records of Amphibia from Tibet, China, with description of *Rhacophorus burmanus*. *Sichuan Journal of Zoology*, **35**(2): 210–216. (in Chinese)
- Kuraishi N, Matsui M, Hamidy A, et al. 2013. Phylogenetic and taxonomic relationships of the *Polypedates leucomystax* complex (Amphibia). *Zoologica Scripta*, **42**(1): 54–70.
- Leaché AD, Reeder TW. 2002. Molecular systematics of the eastern fence lizard (*Sceloporus undulatus*): a comparison of parsimony, likelihood, and Bayesian approaches. *Systematic Biology*, **51**(1): 44–68.
- Li JT, Che J, Bain RH, et al. 2008. Molecular phylogeny of Rhacophoridae (Anura): a framework

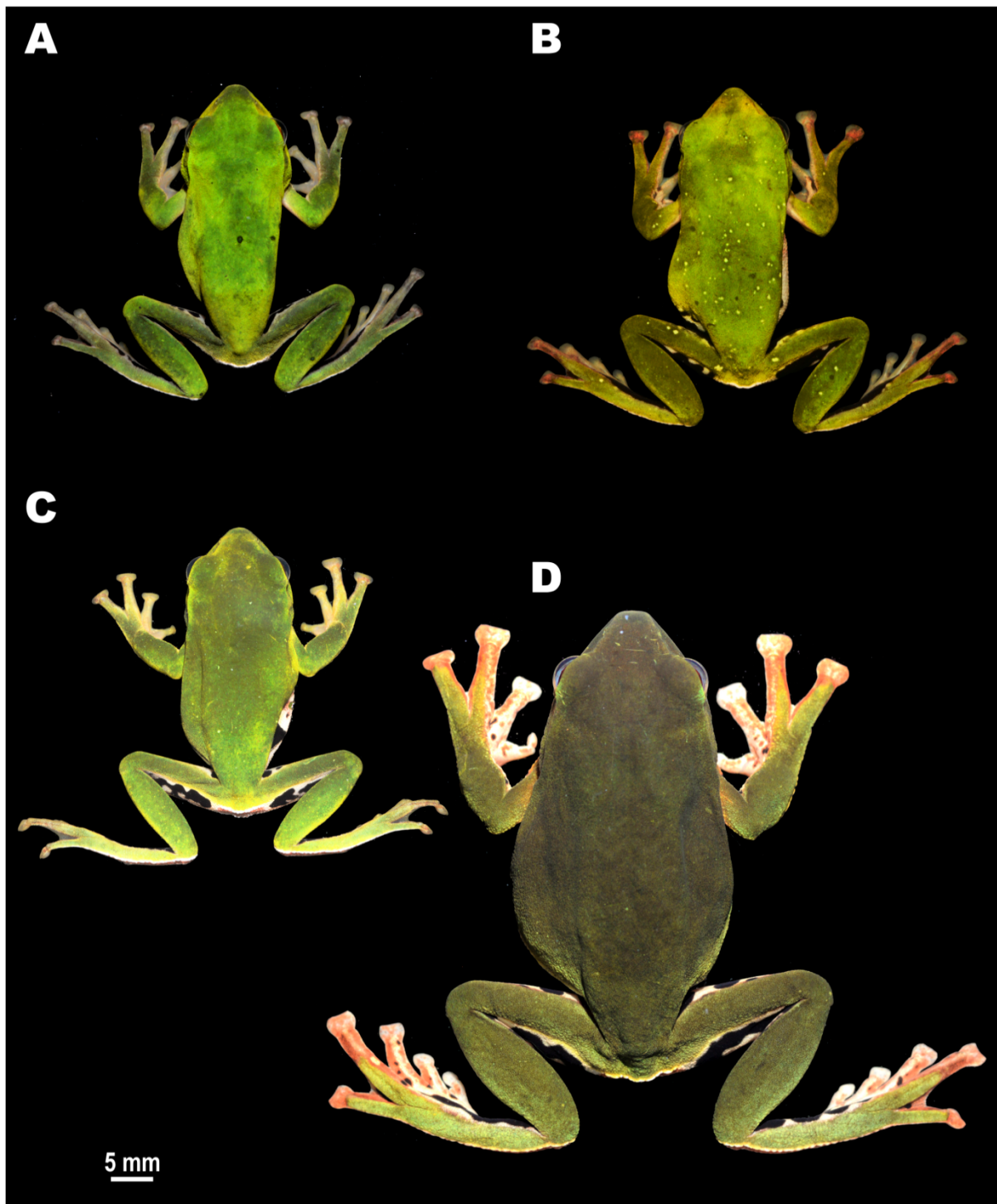
- of taxonomic reassignment of species within the genera *Aquixalus*, *Chiromantis*, *Rhacophorus*, and *Philautus*. *Molecular Phylogenetics and Evolution*, **48**(1): 302–312.
- Li JT, Chen YY, Li SQ, et al. 2011. Catalogue of the type specimens of amphibians and reptiles in the herpetological museum of Chengdu Institute of Biology, Chinese Academy of Sciences: I. Rhacophoridae (Anura, Amphibia). *Asian Herpetological Research*, **2**(3): 129–141.
- Li JT, Liu J, Chen YY, et al. 2012. Molecular phylogeny of treefrogs in the *Rhacophorus dugritei* species complex (Anura: Rhacophoridae), with descriptions of two new species. *Zoological Journal of the Linnean Society*, **165**(1): 143–162.
- Liu BQ, Wang YF, Jiang K, et al. 2017. A new treefrog species of the genus *Rhacophorus* found in Zhejiang, China (Anura: Rhacophoridae). *Chinese Journal of Zoology*, **52**(3): 361–372. (in Chinese)
- Liu S, Hui H, Rao DQ. 2020. First record of *Zhangixalus franki* Ninh, Nguyen, Orlov, Nguyen & Ziegler, 2020 (Anura, Rhacophoridae) from China. *Herpetozoa*, **33**: 185–189.
- Mathipi V, Laltlanhlu LH, Biakzuala L, et al. 2021. On the phylogeny of the Suffry Red-webbed treefrog, *Zhangixalus suffry* (Bordoloi, Bortamuli, and Ohler 2007), with notes on distribution and comparisons with the Giant treefrog, *Zhangixalus smaragdinus* (Blyth 1852), and other closely related species in Mizoram. *Reptiles & Amphibians*, **28**(3): 475–479.
- Matsui M, Kawahara Y, Nishikawa K, et al. 2019. Molecular phylogeny and evolution of two *Rhacophorus* species endemic to mainland Japan. *Asian Herpetological Research*, **10**(2): 86–104.
- Matsui M, Shimada T, Sudin A. 2014. First record of the tree-frog genus *Chiromantis* from Borneo with the description of a new species (Amphibia: Rhacophoridae). *Zoological Science*, **31**(1): 45–51.
- Matsui M, Wu GF. 1994. Acoustic characteristics of treefrogs from Sichuan, China, with comments on systematic relationship of *Polypedates* and *Rhacophorus* (Anura, Rhacophoridae). *Zoological Science*, **11**(3): 485–490.
- Mo YM, Chen WC, Liao XW, et al. 2016. A new species of the genus *Rhacophorus* (Anura: Rhacophoridae) from southern China. *Asian Herpetological Research*, **7**(3): 139–150.
- Murphy RW, Crawford AJ, Bauer AM, et al. 2013. Cold Code: the global initiative to DNA barcode amphibians and nonavian reptiles. *Molecular Ecology Resources*, **13**(2): 161–167.
- Nguyen TT, Matsui M, Eto K, et al. 2014. A preliminary study of phylogenetic relationships and taxonomic problems of Vietnamese *Rhacophorus* (Anura: Rhacophoridae). *Russian Journal of Herpetology*, **21**(4): 274–280.
- Nguyen TT, Ninh HT, Orlov N, et al. 2020. A new species of the genus *Zhangixalus* (Amphibia: Rhacophoridae) from Vietnam. *Journal of Natural History*, **54**(1–4): 257–273.
- Ninh HT, Nguyen TT, Orlov N, et al. 2020. A new species of the genus *Zhangixalus* (Amphibia: Rhacophoridae) from Vietnam. *European Journal of Taxonomy*, (688): 1–18.

- O'Connell KA, Smart U, Smith EN, et al. 2018. Within-island diversification underlies parachuting frog (*Rhacophorus*) species accumulation on the Sunda Shelf. *Journal of Biogeography*, **45**(4): 929–940.
- Ohler A. 2009. *Rhacophorus burmanus* (Anderson, 1939) the valid nomen for *Rhacophorus taroensis* Smith, 1940 and *Rhacophorus gongshanensis* Yang & Su, 1984. *Herpetozoa*, **21**: 179–182.
- Ohler A, Deuti K. 2018. *Polypedates smaragdinus* Blyth, 1852 – a senior subjective synonym of *Rhacophorus maximus* Günther, 1858. *Zootaxa*, **4375**(2): 273–280.
- Ohler A, Marquis O, Swan S, et al. 2000. Amphibian biodiversity of Hoang Lien Nature Reserve (Lao Cai Province, northern Vietnam) with description of two new species. *Herpetozoa*, **13**(1–2): 71–87.
- Orlov NL, Lathrop A, Murphy RW, et al. 2001. Frogs of the family Rhacophoridae (Anura: Amphibia) in the northern Hoang Lien Mountains (Mount Fan Si Pan, Sa Pa District, Lao Cai Province), Vietnam. *Russian Journal of Herpetology*, **8**(1): 17–44.
- Orlov NL, Murphy RW, Ananjeva NB, et al. 2002. Herpetofauna of Vietnam, a checklist. Part I. Amphibia. *Russian Journal of Herpetology*, **9**(2): 81–104.
- Orton GL. 1953. The systematics of Vertebrate larvae. *Systematic Zoology*, **2**(2): 63–75.
- Pan T, Zhang YN, Wang H, et al. 2017. A new species of the genus *Rhacophorus* (Anura: Rhacophoridae) from Dabie Mountains in East China. *Asian Herpetological Research*, **8**(1): 1–13.
- Posada D, Crandall KA. 1998. MODELTEST: testing the model of DNA substitution. *Bioinformatics*, **14**(9): 817–818.
- Poyarkov NA, Kropachev II, Gogoleva SS, et al. 2018. A new species of the genus *Theloderma* Tschudi, 1838 (Amphibia: Anura: Rhacophoridae) from Tay Nguyen Plateau, central Vietnam. *Zoological Research*, **39**(3): 158–184.
- Poyarkov NA, Orlov NL, Moiseeva AV, et al. 2015. Sorting out moss frogs: mtDNA data on taxonomic diversity and phylogenetic relationships of the Indochinese species of the genus *Theloderma* (Anura, Rhacophoridae). *Russian Journal of Herpetology*, **22**(4): 241–280.
- Rao DQ, Wilkinson JA, Liu HN. 2006. A new species of *Rhacophorus* (Anura: Rhacophoridae) from Guangxi Province, China. *Zootaxa*, **1258**(1): 17–31.
- Ronquist F, Huelsenbeck JP. 2003. MrBayes 3: Bayesian phylogenetic inference under mixed models. *Bioinformatics*, **19**(12): 1572–1574.
- Sambrook JF, Russell DW. 2001. *Molecular Cloning: A Laboratory Manual*. 3rd ed. Cold Spring Harbor: Cold Spring Harbor Laboratory Press.
- Savage JM. 1975. Systematics and distribution of the Mexican and Central American stream frogs related to *Eleutherodactylus rugulosus*. *Copeia*, **1975**(2): 254–306.
- Tamura K, Stecher G, Peterson D, et al. 2013. MEGA6: molecular evolutionary genetics analysis version 6.0. *Molecular Biology and Evolution*, **30**(12): 2725–2729.

- Thompson JD, Gibson TJ, Plewniak F, et al. 1997. The CLUSTAL_X windows interface: flexible strategies for multiple sequence alignment aided by quality analysis tools. *Nucleic Acids Research*, **25**(24): 4876–4882.
- Vences M, Thomas M, Bonett RM, et al. 2005a. Deciphering amphibian diversity through DNA barcoding: chances and challenges. *Philosophical Transactions of the Royal Society B: Biological Sciences*, **360**(1462): 1859–1868.
- Vences M, Thomas M, van der Meijden A, et al. 2005b. Comparative performance of the 16S rRNA gene in DNA barcoding of amphibians. *Frontiers in Zoology*, **2**(1): 5.
- Vieites DR, Wollenberg KC, Andreone F, et al. 2009. Vast underestimation of Madagascar's biodiversity evidenced by an integrative amphibian inventory. *Proceedings of the National Academy of Sciences of the United States of America*, **106**(20): 8267–8272.
- Wang JC, Cui JG, Shi HT, et al. 2012. Effects of body size and environmental factors on the acoustic structure and temporal rhythm of calls in *Rhacophorus dennysi*. *Asian Herpetological Research*, **3**(3): 205–212.
- Wassersug RJ, Frogner KJ, Inger RF. 1981. Adaptations for life in tree holes by rhacophorid tadpoles from Thailand. *Journal of Herpetology*, **15**(1): 41–52.
- Yu GH, Hui H, Hou M, et al. 2019. A new species of *Zhangixalus* (Anura: Rhacophoridae), previously confused with *Zhangixalus smaragdinus* (Blyth, 1852). *Zootaxa*, **4711**(2): 275–292.
- Yu GH, Rao DQ, Yang JX, et al. 2008. Phylogenetic relationships among Rhacophorinae (Rhacophoridae, Anura, Amphibia), with an emphasis on the Chinese species. *Zoological Journal of the Linnean Society*, **153**(4): 733–749.
- Zhang J, Jiang K, Hou M. 2011. *Rhacophorus dorsovireidis* Bourret, a new record of family Rhacophoridae to China. *Acta Zootaxonomica Sinica*, **36**(4): 986–989. (in Chinese)



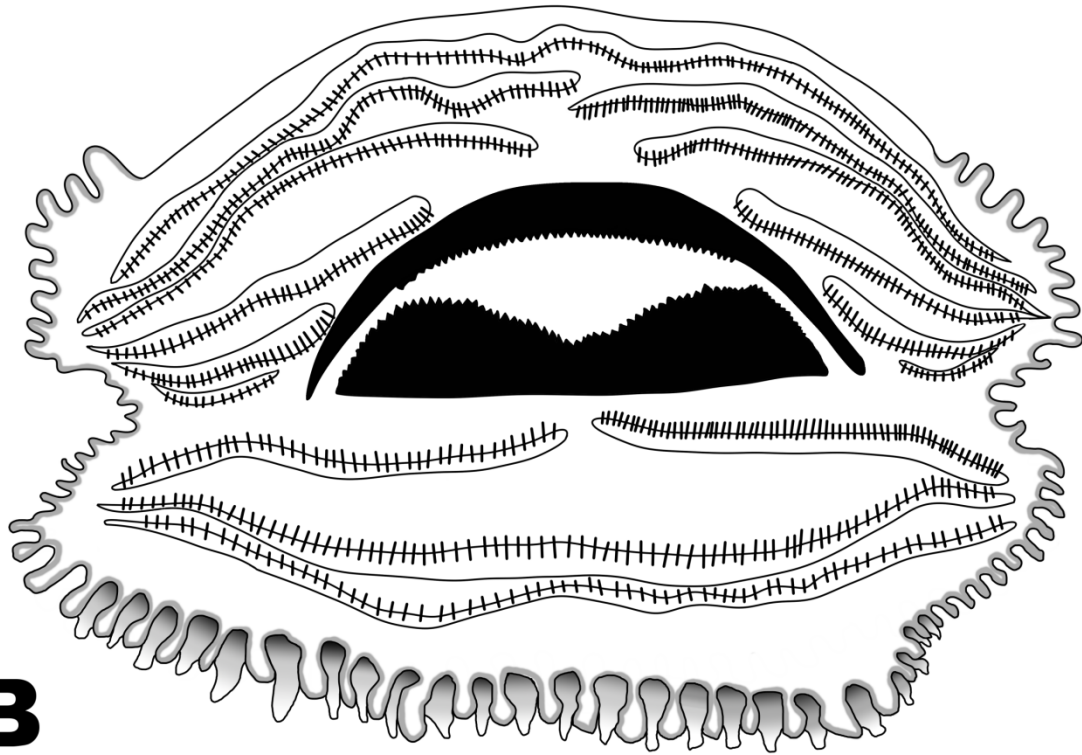
Supplementary Figure S1 Life coloration of the holotype of *Zhangixalus melanoleucus* sp. nov. (AUP02505), adult male, in (A) Dorsal view; (B) ventral view; (C) head lateral view; (D) volar view of left hand; (E) plantar view of left foot. Scale bar equals 5 mm. Photographs by N. A. Poyarkov.



Supplementary Figure S2 Variation in life dorsal coloration within the type series of *Zhangixalus melanoleucus* **sp. nov.** (A) AUP 02506, adult male; (B) ZMMU A-7781, adult male; (C) AUP 02507, adult male; (D) ZMMU A-7782, adult female. Scale bar equals 5 mm. Photographs by N. A. Poyarkov.



Supplementary Figure S3 Amplexus of *Zhangixalus melanoleucus* sp. nov. (ZMMU A-7781 male and ZMMU A-7782 female). Photograph by P. Pawangkhanant.



Supplementary Figure S4 Tadpole of *Zhangixalus melanoleucus* **sp. nov.** (ZMMU A-7783-1) (Gosner stage 35). (A) In dorsolateral view in situ, photograph by P. Pawangkhanant; (B) oral disk morphology, drawing by S. Idiiatullina.



Supplementary Figure S5 Male *Zhangixalus nigropunctatus* (Liu, Hu & Yang) from Yushe National Forest Park (N 26.46 °, E 104.81 °, elevation 2070 m a.s.l.), Guizhou Province, China, in life; photograph by Jian Wang.

Supplementary Table S1. Localities, voucher information, and GenBank accession numbers for all specimens used in molecular analyses in this study. For references see Supplementary materials and methods section. (n.a. - not available)

Species	Specimen ID	12S-16S	COI	Locality	Reference
<i>Z. melanoleucus</i> sp. nov.	BEI 01010	OQ305233	OQ288104	Phou Samsoum Mt., Xiengkhoang, Laos	<i>this study</i>
<i>Z. melanoleucus</i> sp. nov.	BEI 01011	OQ305235	OQ288106	Phou Samsoum Mt., Xiengkhoang, Laos	<i>this study</i>
<i>Z. melanoleucus</i> sp. nov.	AUP 02507	OQ305236	OQ288107	Phou Samsoum Mt., Xiengkhoang, Laos	<i>this study</i>
<i>Z. melanoleucus</i> sp. nov.	ZMMU A-7781	OQ305234	OQ288105	Phou Samsoum Mt., Xiengkhoang, Laos	<i>this study</i>
<i>Z. achantharrhena</i>	ENS 7597	MF066239	n.a.	Indonesia	O'Connell et al. (2018)
<i>Z. amamiensis</i>	KUHE 22524	LC386575	LC386524	Amamioshima, Japan	Matsui et al. (2019)
<i>Z. arboreus</i>	KUHE 47945	LC386562	LC386500	Iida-shi, Nagano, Japan	Matsui et al. (2019)
<i>Z. arvalis</i>	17560	OQ297601	MH034328	Douliu, Yunlin, Taiwan, China	Jang-Liaw unpublished data
<i>Z. burmanus</i>	SCUM 060614L	EU215537	KP996738	Mt Gaoligong, Yunnan, China	Li et al. (2008)
<i>Z. chenfui</i>	Li05	JX219432	KP996815	Emeishan, Sichuan, China	Li et al. (2012)
<i>Z. dennysi</i>	RDEN 20150618	KT191129	n.a.	Ningguo, Meilin, Anhui, China	Huang et al. (2016)
<i>Z. dorsovireidis</i>	ROM 38015	JX219423	n.a.	Sa Pa, Lao Cai, Vietnam	Li et al. (2012)
<i>Z. duboisi</i>	KIZ 060821289	EF564567	EF564567	Jinping, Yunnan, China	Yu et al. (2008)
<i>Z. dugritei</i>	KUHE 27701	LC010584	n.a.	Emeishan, Sichuan, China	Nguyen et al. (2014)
<i>Z. dulitensis</i>	BORNEENSIS 09087	AB847123	KP996755	Sabah, Borneo, Malaysia	Matsui et al. (2014)
<i>Z. feae</i>	SCUM 050642W	EU215544	KP996749	Daweishan, Pingbian, Yunnan, China	Li et al. (2008)
<i>Z. franki</i>	VNMN 011686	LC548745	n.a.	Tung Vai, Quan Ba, Ha Giang, Vietnam	Ninh et al. (2020)
<i>Z. gongshanensis</i>	KIZ 1049	EF564569	EF564569	Gongshan, Yunnan, China	Yu et al. (2008)
<i>Z. hongchibaensis</i>	CIB 097696	JN688882	n.a.	Hongchiba, Wuxi, Chongqing, China	Li et al. (2012)
<i>Z. hui</i>	SCUM 0504111L	JN688878	KP996701	Yanwotang, Zhaojue, Sichuan, China	Li et al. (2012)
<i>Z. hungfuensis</i>	SCUM 060425L	EU215538	LC386532	Wenchuan, Sichuan, China	Li et al. (2008)

<i>Z. jodiae</i>	VNMN 07122	LC545595	n.a.	Tung Vai, Quan Ba, Ha Giang, Vietnam	Nguyen et al. (2020)
<i>Z. lishuiensis</i>	YPX 47791	KY653718	n.a.	Lishui, Zhejiang, China	Liu et al. (2017)
<i>Z. minimus</i>	KUHE 70049	LC386569	LC386532	China	Matsui et al. (2019)
<i>Z. moltrechti</i>	KUHE 31070	LC386570	LC386533	Taipei, Taiwan, China	Matsui et al. (2019)
<i>Z. nigropunctatus</i>	GZ 070658	JX219430	JN700897	Weining, Guizhou, China	Li et al. (2012)
<i>Z. omeimontis</i>	CIB 20060104	LC010595	LC386536	Sichuan, China	Nguyen et al. (2014)
<i>Z. owstoni</i>	KUHE 12764	LC386572	LC386537	Ishigakijima, Japan	Matsui et al. (2019)
<i>Z. pachyproctus</i>	KUHE 35130	LC386568	LC386531	Pilok, Thailand	Matsui et al. (2019)
<i>Z. pingbianensis</i>	YN 080484	JX219418	KP996808	Pingbian, Yunnan, China	Li et al. (2012)
<i>Z. pinglongensis</i>	NHMG 201002011	KU170684	n.a.	Pinglongshan, Shangsi, Guangxi, China	Mo et al. (2016)
<i>Z. prominanus</i>	Rao 081201	JX219434	LC386529	Malaysia	Li et al. (2012)
<i>Z. puerensis</i>	SCUM 060649L	EU215542	KP996810	Puer, Yunnan, China	Li et al. (2008)
<i>Z. schlegelii</i>	KUHE 45531	LC369670	LC386405	Okayama, Japan	Matsui et al. (2019)
<i>Z. smaragdinus</i>	KUHE 34511	LC386567	LC386530	Kachin, Myanmar	Matsui et al. (2019)
<i>Z. suffry</i>	MZMU1390	MT808304	n.a.	Mizoram, India	Lalremsanga et al. unpublished data
<i>Z. taipeianus</i>	KUHE 34347	LC386574	LC386539	Taipei, Taiwan, China	Matsui et al. (2019)
<i>Z. taronensis</i>	SCUM 060614L	EU215537	n.a.	Gaoligong Mt., Yunnan, China	Li et al. (2008)
<i>Z. viridis</i>	KUHE 35354	LC386576	LC386525	Okinawajima, Okinawa, Japan	Matsui et al. (2019)
<i>Z. wui</i>	CIB 097685	JN688881	KP996819	Hanchi, Lichuan, Hubei, China	Li et al. (2012)
<i>Z. yaoshanensis</i>	NHMG 150408	MG322122	n.a.	Jinxiu, Guangxi, China	Chen et al. (2018)
<i>Z. zhokaiyae</i>	AHU-RhaDb-150418-02	KU601494	n.a.	Qianping, Jinzhai, Anhui, China	Pan et al. (2017)
Outgroup					
<i>Leptomantis gauni</i>	FMNH 273928	JX219456	n.a.	Bintulu, Sarawak, Malaysia	Li et al. (2012)
<i>Rhacophorus kio</i>	SCUM 37941C	EU215532	KR087903	Xishuangbanna, Yunnan, China	Li et al. (2008)
<i>Polypedates leucomystax</i>	KUHE 33881	AB728168	n.a.	Chatthin, Sagaing, Myanmar	Kuraishi et al. (2013)

Supplementary Table S2. Uncorrected *p*-distance (percentage) 16S rRNA sequences of *Zhangixalus* species included in phylogenetic analyses (below diagonal), average intraspecific genetic *p*-distances (on diagonal), and standard error estimates (above diagonal).

Taxon	1	2	3	4	5	6	7	8	9	10	11	12	13	14	15	16	17	18	19	20	21	22	23	24	25	
1 <i>Z. melanoleucus</i> sp. nov.	0.0																									
2 <i>Z. dugritei</i>	4.5	–																								
3 <i>Z. hui</i>	4.3	0.2	–																							
4 <i>Z. minimus</i>	4.9	1.4	1.6	–																						
5 <i>Z. hongchibaensis</i>	5.4	1.4	1.6	1.8	–																					
6 <i>Z. hungfuensis</i>	5.8	2.3	2.0	2.5	1.8	–																				
7 <i>Z. wui</i>	5.6	2.0	1.8	2.7	2.5	1.8	–																			
8 <i>Z. puerensis</i>	5.8	2.3	2.0	2.7	2.3	2.3	2.5	–																		
9 <i>Z. amamiensis</i>	5.4	2.9	2.7	3.6	2.7	2.7	2.9	2.3	–																	
10 <i>Z. moltrechti</i>	4.7	2.9	2.7	3.6	3.2	3.4	3.6	3.2	3.2	–																
11 <i>Z. owstoni</i>	4.7	3.8	3.6	4.5	4.0	4.0	4.3	4.0	3.2	1.8	–															
12 <i>Z. taipeianus</i>	5.2	2.9	2.7	4.0	3.2	4.0	3.8	3.2	3.4	2.9	4.3	–														
13 <i>Z. duboisi</i>	5.2	3.4	3.6	4.0	3.2	3.6	3.8	3.6	2.5	3.4	4.3	2.7	–													
14 <i>Z. pingbianensis</i>	5.5	3.5	3.7	4.2	3.5	4.0	3.7	3.7	2.7	3.5	4.5	2.7	0.0	–												
15 <i>Z. omeimontis</i>	5.4	3.6	3.4	4.3	3.4	3.4	3.6	3.4	2.5	3.2	4.0	2.9	0.7	0.8	–											
16 <i>Z. gongshanensis</i>	4.5	3.8	3.5	4.5	4.3	4.8	4.5	4.5	3.5	3.5	4.0	3.3	2.3	2.3	2.5	–										
17 <i>Z. burmanus</i>	4.3	3.4	3.2	4.0	4.0	4.5	4.3	4.0	3.4	3.2	3.6	2.9	2.3	2.2	2.5	0.0	–									
18 <i>Z. taronensis</i>	4.3	3.4	3.2	4.0	4.0	4.5	4.3	4.0	3.4	3.2	3.6	2.9	2.3	2.2	2.5	0.0	0.0	–								
19 <i>Z. franki</i>	4.0	3.2	2.9	3.8	3.8	3.8	3.6	3.4	2.7	3.4	3.4	2.9	1.6	1.5	1.8	1.3	1.1	1.1	–							
20 <i>Z. schlegelii</i>	6.5	4.7	4.5	5.4	4.5	4.7	5.2	4.5	4.3	4.7	5.6	4.0	4.9	5.2	4.9	4.5	4.3	4.3	4.3	–						
21 <i>Z. viridis</i>	5.4	3.2	2.9	3.6	3.2	3.6	3.8	2.7	2.7	2.9	4.3	2.7	3.6	3.7	3.4	4.0	3.6	3.6	3.8	4.3	–					
22 <i>Z. arboreus</i>	4.7	3.4	3.2	3.6	3.6	3.8	4.0	3.6	3.6	2.5	3.8	2.7	3.2	3.2	2.9	3.0	2.7	2.7	3.4	4.3	2.3	–				

(Continued on the next page)

Supplementary Table S2. (Continued)

Taxon	1	2	3	4	5	6	7	8	9	10	11	12	13	14	15	16	17	18	19	20	21	22	23	24	25
23 <i>Z. dorsoviridis</i>	5.8	4.9	5.2	5.6	4.7	4.3	5.4	5.2	4.0	4.9	5.4	4.3	2.9	3.2	3.6	4.5	4.3	4.3	4.0	5.4	4.3	3.4	–		
24 <i>Z. zhokaiyae</i>	6.3	5.3	5.1	6.0	5.8	4.9	5.3	4.9	3.9	5.1	5.1	3.9	3.9	4.1	4.2	4.9	4.4	4.4	4.2	5.6	4.2	3.5	2.6	–	
25 <i>Z. lishuiensis</i>	5.8	5.2	5.2	5.6	5.4	4.7	5.4	4.9	3.8	4.9	4.9	4.3	3.6	3.7	4.0	4.8	4.3	4.3	4.0	5.4	4.0	3.4	2.0	1.2	–
26 <i>Z. pachyproctus</i>	6.3	6.3	6.1	6.1	6.5	6.5	6.7	6.3	5.8	5.4	6.3	5.6	6.1	6.5	5.8	6.3	5.6	5.6	6.3	7.2	4.5	4.5	5.8	5.1	4.9
27 <i>Z. dennysi</i>	6.5	6.1	5.8	6.3	6.3	6.5	5.8	5.8	5.6	6.1	6.3	6.3	6.1	6.5	6.3	6.5	5.8	5.8	5.4	7.0	4.7	6.3	7.0	7.2	7.0
28 <i>Z. suffry</i>	8.8	9.7	9.4	9.7	9.2	9.0	9.7	8.5	8.3	8.3	8.3	8.5	8.3	8.7	8.3	8.8	8.3	8.3	8.1	8.3	8.3	7.9	9.2	7.0	8.3
29 <i>Z. smaragdinus</i>	8.5	9.0	8.8	9.2	8.5	8.8	9.4	7.9	7.6	8.1	8.1	8.3	8.1	8.7	8.1	9.3	8.5	8.5	8.3	8.5	8.1	7.4	8.5	6.3	7.6
30 <i>Z. feae</i>	4.0	4.7	4.5	4.9	4.5	4.9	5.2	3.8	4.0	3.6	4.9	3.2	4.0	4.2	4.3	4.0	3.6	3.6	3.8	4.9	3.4	3.2	4.5	3.9	4.0
31 <i>Z. chenfui</i>	5.6	6.5	6.3	7.2	6.7	6.5	6.1	5.6	5.2	5.4	5.2	5.6	6.1	6.5	6.1	5.8	5.4	5.4	5.2	6.1	5.6	5.8	6.5	6.0	6.1
32 <i>Z. nigropunctatus</i>	3.4	5.9	5.6	6.1	6.1	6.5	6.8	6.5	5.4	4.7	5.0	5.2	4.3	4.8	4.5	3.5	3.4	3.4	3.4	7.0	6.5	5.2	5.9	6.7	6.3
33 <i>Z. yaoshanensis</i>	4.9	6.5	6.3	6.3	6.7	6.7	7.4	6.3	5.4	6.1	6.3	6.1	5.6	6.2	5.8	5.3	5.2	5.2	4.7	7.4	6.7	6.5	6.7	7.0	6.7
34 <i>Z. pinglongensis</i>	4.5	5.4	5.2	5.4	5.8	5.8	6.5	5.4	5.4	4.9	5.8	4.3	4.3	4.7	4.5	4.8	4.5	4.5	4.0	7.0	5.8	5.2	5.8	6.3	6.1
35 <i>Z. achantharrhena</i>	7.4	7.9	7.6	8.5	8.3	8.5	7.9	7.6	7.2	7.4	6.5	7.4	7.2	7.7	7.4	6.8	6.3	6.3	6.1	9.0	7.9	8.1	8.5	8.8	8.8
36 <i>Z. dulitensis</i>	6.7	6.5	6.3	6.7	7.0	6.7	6.5	6.3	5.8	6.1	6.1	5.6	6.3	6.7	6.5	6.5	6.1	6.1	6.1	7.6	6.5	6.1	6.7	6.5	6.5
37 <i>Z. prominanus</i>	6.3	7.2	7.0	7.4	7.9	7.4	7.2	6.5	6.1	6.7	6.7	5.2	5.6	6.0	5.8	5.8	5.4	5.4	4.9	8.1	6.3	6.3	7.2	6.5	6.7
38 <i>Z. arvalis</i>	8.3	8.3	8.5	8.3	7.0	8.3	8.5	8.1	7.6	8.8	9.2	8.1	7.6	7.7	8.1	8.5	8.5	8.5	8.3	10.1	7.9	9.4	9.0	9.5	9.4
39 <i>Leptomantis gauni</i>	9.5	9.5	9.2	9.7	8.8	9.0	9.2	9.0	7.9	9.2	8.8	8.3	9.5	10.0	9.5	9.3	8.8	8.8	8.8	7.9	8.3	8.8	9.5	9.8	9.7
40 <i>Rhacophorus kio</i>	11.0	10.8	10.6	11.2	11.2	10.6	11.0	11.2	10.8	9.4	8.8	10.8	11.5	12.2	11.5	11.3	10.6	10.6	11.0	11.7	11.0	10.8	11.9	11.8	12.1
41 <i>Polypedates leucomystax</i>	14.7	16.3	16.3	15.8	16.7	16.7	16.3	16.0	16.3	14.9	14.7	16.0	15.4	16.0	15.8	16.3	15.6	15.6	15.4	16.0	16.0	16.3	15.4	16.1	14.7

(Continued on the next page)

Supplementary Table S2. (Continued)

Taxon	26	27	28	29	30	31	32	33	34	35	36	37	38	39	40	41
26 <i>Z. pachyproctus</i>	–															
27 <i>Z. dennysi</i>	7.0	–														
28 <i>Z. suffry</i>	8.1	9.7	–													
29 <i>Z. smaragdinus</i>	7.6	9.7	1.6	–												
30 <i>Z. feae</i>	4.3	5.6	6.7	6.5	–											
31 <i>Z. chenfui</i>	7.2	7.6	8.3	8.3	4.7	–										
32 <i>Z. nigropunctatus</i>	7.0	7.2	9.2	8.8	5.4	6.3	–									
33 <i>Z. yaoshanensis</i>	7.6	8.3	9.0	9.0	5.6	5.8	4.1	–								
34 <i>Z. pinglongensis</i>	6.7	7.9	8.5	8.3	4.7	6.3	4.1	3.4	–							
35 <i>Z. achantharrhena</i>	8.8	7.6	9.4	9.2	7.0	7.2	7.9	8.3	7.9	–						
36 <i>Z. dulitensis</i>	7.0	8.3	9.4	8.8	5.6	7.0	6.8	7.6	7.0	3.4	–					
37 <i>Z. prominanus</i>	7.4	7.9	9.0	9.2	5.8	6.3	6.3	6.7	5.6	4.5	2.9	–				
38 <i>Z. arvalis</i>	8.1	7.4	10.1	10.3	7.9	9.4	8.6	9.7	9.4	9.4	9.9	9.7	–			
39 <i>Leptomantis gauni</i>	9.5	10.4	10.4	10.4	7.9	8.8	10.4	11.0	10.6	9.5	8.6	9.7	9.9	–		
40 <i>Rhacophorus kio</i>	11.9	11.0	13.9	13.7	11.7	10.8	11.5	12.8	12.1	10.3	10.6	11.7	13.0	11.0	–	
41 <i>Polypedates leucomystax</i>	14.5	15.8	16.9	17.2	16.0	16.5	14.7	15.8	14.7	14.7	15.4	15.4	15.4	16.0	15.1	–

Supplementary Table S3. Measurements of the type series (in mm) of *Zhangixalus melanoleucus* sp. nov.

Specimen ID	BEI 01010	BEI 01011	ZMMU A-7781	AUP 02507	Min–Max (4 males)	Mean±SD (4 males)	ZMMU A-7782
Type	Holotype	Paratype	Paratype	Paratype			Paratype
Sex	Male	Male	Male	Male			Female
SVL	35.0	34.4	36.3	34.4	34.4–36.3	35.03±0.88	53.7
A-G	17.8	17.6	17.9	18.3	17.6–18.3	17.89±0.29	26.8
HW	13.3	12.2	13.4	12.0	12.0–13.4	12.72±0.71	19.5
HL	13.6	12.6	13.3	12.0	12.0–13.6	12.87±0.69	18.7
HD	6.8	7.1	7.8	6.0	6.0–7.8	6.94±0.75	10.8
UEW	3.2	3.0	3.1	3.1	3.0–3.2	3.12±0.12	4.0
IOD	4.7	4.1	4.8	4.2	4.1–4.8	4.43±0.37	6.3
ED	4.6	4.2	4.7	4.1	4.1–4.7	4.39±0.29	6.6
TD	2.3	1.9	2.2	1.9	1.9–2.3	2.05±0.21	3.0
ESL	6.1	5.8	6.1	5.4	5.4–6.1	5.85±0.36	7.7
IND	4.3	4.2	4.4	4.2	4.2–4.4	4.28±0.09	6.5
END	2.4	2.0	2.6	2.4	2.0–2.6	2.35±0.26	3.9
TED	1.0	0.9	1.0	1.0	0.9–1.0	0.98±0.08	1.5
NS	3.6	3.9	3.8	3.7	3.6–3.9	3.74±0.13	4.0
FLL	27.3	25.4	25.4	24.8	24.8–27.3	25.72±1.08	37.7
HML	7.5	7.1	6.8	7.1	6.8–7.5	7.09±0.29	9.2
LAL	8.3	7.5	8.0	7.4	7.4–8.3	7.80±0.43	11.4
ML	11.5	10.8	10.7	10.3	10.3–11.5	10.83±0.50	17.0
1FLi	5.2	5.1	4.9	5.0	4.9–5.2	5.04±0.13	7.6
1FLo	4.1	3.6	3.8	3.5	3.5–4.1	3.73±0.26	5.1
2FLi	5.4	5.6	5.2	5.3	5.2–5.6	5.36±0.18	8.7

3FLi	7.8	8.3	7.9	7.8	7.8–8.3	8.00±0.22	11.8
4FLi	6.2	6.6	7.0	5.7	5.7–7.0	6.39±0.57	10.0
FTD	2.4	2.0	2.5	2.3	2.0–2.5	2.28±0.21	3.9
NPL	2.2	2.4	3.0	2.0	2.0–3.0	2.38±0.44	0.0
MCTe	0.8	0.9	1.0	0.7	0.7–1.0	0.84±0.14	2.0
HLL	50.8	49.1	51.2	47.4	47.4–51.2	49.63±1.74	73.6
FL	12.3	12.4	13.0	12.1	12.1–13.0	12.43±0.39	18.8
TL	14.7	14.0	14.3	13.8	13.8–14.7	14.18±0.36	21.6
TTL	8.0	7.8	8.0	7.2	7.2–8.0	7.75±0.35	10.8
FOT	15.9	14.9	16.0	14.3	14.3–16.0	15.28±0.83	22.3
1TLi	5.1	4.5	5.9	4.5	4.5–5.9	5.01±0.64	8.6
1TL _o	2.7	2.5	3.2	2.2	2.2–3.2	2.63±0.42	3.6
2TLi	5.2	4.7	5.5	5.2	4.7–5.5	5.14±0.34	6.8
3TLi	7.2	6.7	6.9	6.6	6.6–7.2	6.84±0.28	9.9
4TLi	8.5	8.2	8.8	8.9	8.2–8.9	8.62±0.32	13.1
5TLi	6.4	5.7	6.0	5.8	5.7–6.4	5.97±0.31	9.5
HTD	2.2	1.8	2.2	1.8	1.8–2.2	2.01±0.24	3.0
MTTi	1.9	1.8	1.9	1.7	1.7–1.9	1.81±0.09	3.1
IMW	1.2	1.2	1.2	1.3	1.2–1.3	1.21±0.05	2.3

Supplementary Table S4. Measurements of the series of *Zhangixalus melanoleucus* **sp. nov.** tadpoles (ZMMU A-7783; all in mm). For character abbreviations see Supplementary materials and methods.

Character	ZMMU A-7783-1	ZMMU A-7783-2	ZMMU A-7783-3
TL	39.8	37.0	25.1
BL	17.0	16.7	12.9
TaL	22.8	20.4	12.1
BW	9.5	10.2	8.1
BH	8.1	7.5	5.5
TH	9.3	10.9	7.2
SVL	18.7	17.4	13.9
SSp	10.0	7.0	6.6
UF	2.7	3.4	2.0
LF	2.1	2.5	1.4
IN	2.7	2.6	2.2
IP	6.1	6.0	3.7
RN	0.9	1.2	1.0
NP	2.6	2.3	2.0
ED	1.9	2.0	1.1
ODW	3.2	2.6	2.2
LTRF	1:5+5/1+1:2	1:5+5/1+1:2	1:5+5/1+1:2

Supplementary Table S5. Basic morphological characters for the species of *Zhangixalus* distributed in Indochina, China, India and Myanmar as compared to *Zhangixalus melanoleucus* **sp. nov.** Symbol characters are: ① SVL in males (mm); ② SVL in females (mm); ③ Color of iris; ④ Finger webbing; ⑤ Colorations on dorsum; ⑥ Colorations on ventral; ⑦ Colorations on flank; ⑧ Colorations on thigh; ‘?’: no data.

Species	①	②	③	④	⑤	⑥
<i>melanoleucus</i> sp. nov.	34.4–36.3	53.7	reddish orange	reduced	immaculate green	immaculate white
<i>burmanus</i>	47.0–59.5	64.2–77.3	yellow	reduced	green/dark green with small pale yellow/brown/dark dots	cream with small pale yellow
<i>chenfui</i>	32.7–40.5	46.0–55.0	reddish-orange	reduced	immaculate green	cream with small pale yellow
<i>dennysi</i>	68–92	83–109	yellowish-gold	reduced	green with small brown spots	immaculate cream
<i>dorsoviridis</i>	31.3–42.4	37.9–42.8	reddish-white	reduced	immaculate green	cream to orange without spots
<i>duboisi</i>	61.5–65.7	71.1–74.1	yellowish-gold	reduced	green with red-brown spots	fleshy with brown spots
<i>dugritei</i>	41.5–45.4	57.7–64.3	yellowish-brown	reduced	green with round spots of a golden metallic ash	cream yellow with dark grey
<i>feae</i>	86–111	68–118	green-gold	complete	immaculate green	anteriorly white, posteriorly pinkish, pale green throat
<i>franki</i>	77.9–85.8	?	bronze	reduced	green with dark brown spots	immaculate grey
<i>hongchibaensis</i>	46.5–49.7	55.3	yellowish-brown	reduced	yellowish brown spots edged with dark brown	creamy white with vaguely greyish brown blotches
<i>hui</i>	40.0–45.4	51.0–66.0	reddish-brown	reduced	green with brow spots	cream/yellow with dark grey
<i>hungfuensis</i>	30.8–36.8	45.5	green-gold	reduced	green with small white spots	pinkish with pale yellow
<i>jodiae</i>	36.1–39.8	?	silver	reduced	immaculate green	immaculate cream
<i>leucofasciatus</i>	47.5–49.4	?	yellowish-brown	reduced	immaculate green	immaculate white
<i>lishuiensis</i>	34.2–35.8	45.9	yellowish-gold	reduced	immaculate pure green	anteriorly white, posteriorly yellow without spots
<i>minimus</i>	28.1	37	yellowish-gold	reduced	immaculate green	immaculate cream/grey

<i>nigropunctatus</i>	32.0–37.0	44.0–45.0	yellowish-gold	reduced	immaculate green	immaculate white
<i>omeimontis</i>	52–66	70–80	yellowish-gold	reduced	green with brown interweave patterns	cream with very small dark spots
<i>pachyproctus</i>	73.4–78.2	102.4	yellowish-gold	complete	immaculate green	immaculate light brown/white
<i>pinglongensis</i>	32–38.5	?	silvery	reduced	immaculate green	immaculate white
<i>puerensis</i>	35.5–41	52–55.2	yellowish-gold	reduced	green with brownish-red spots	white with small spots
<i>smaragdinus</i>	57.0–84.0	85.0–112.0	yellowish-gold	complete	immaculate green	immaculate light brown/white
<i>wui</i>	35.2–38.2	48.6	grayish-gold	reduced	numerous light-brown spots with dark yellowish brown edges	creamy white with vague greyish brown blotches
<i>yaoshanensis</i>	31.6–36.4	49.2–51.1	grayish-gold	reduced	immaculate green	immaculate cream
<i>yinggelingensis</i>	43.0–43.4	?	grayish-gold	reduced	green with few fine white spots	immaculate yellowish
<i>zhoukaiyae</i>	27.9–37.1	41.1–44.7	yellowish-gold	reduced	immaculate green	immaculate pure paler yellowish

(Continued on the next page)

Supplementary Table S5. (Continued)

Species	⑦	⑧	Sources
<i>melanoleucus</i> sp. nov	white with irregular black pattern	white with irregular black pattern	18
<i>burmanus</i>	with small brown/yellow/dark blotches	cream with scattered mottling	8
<i>chenfui</i>	grey without blotches	grey without blotches	5
<i>dennysi</i>	cream/gray with small white spots	cream without blotches	5, 18
<i>dorsoviridis</i>	white with variable black spots	cream with small black spots	2, 18
<i>duboisii</i>	blackish with white spots	white with dark brown marbling	1, 7
<i>dugritei</i>	marbled with cream yellow	marbled with cream yellow	5, 7
<i>feae</i>	uniform green without blotches	uniform green without blotches	5, 18
<i>franki</i>	with a white stripe, separating upper green part from lower cream part	immaculate grey	16,17
<i>hongchibaensis</i>	light green with numerous large spots of light yellowish	lightly red, marbled with grey	7
<i>hui</i>	marbled with cream yellow	marbled with cream yellow	7
<i>hungfuensis</i>	cream without blotches	grey without blotches	5
<i>jodiae</i>	cream with irregular black and orange blotches	black blotches interposed by orange	15
<i>leucofasciatus</i>	cream with wide white band in middle	gray without blotches	5
<i>lishuiensis</i>	cream without blotches	gray without blotches	10
<i>minimus</i>	grey with narrow white band in middle	cream with scattered mottling	3, 5
<i>nigropunctatus</i>	green above, white below with small black spots in posteriorly	cream/yellowish with black blotches	5
<i>omeimontis</i>	dark brow mottling	dark brow without blotches	5
<i>pachyproctus</i>	cream/grey scattered with clouded light brown spots	cream/grey scattered with cloudy light brown	14, 18

<i>pinglongensis</i>	black blotches with white spots	spots black blotches with white spots and faint orange tint	9
<i>puerensis</i>	black with irregular white pattern	black with irregular white pattern	7, 18
<i>smaragdinus</i>	cream/grey scattered with clouded light brown spots	cream/grey scattered with cloudy light brown spots	13, 14
<i>wui</i>	light green with numerous light-brown spots	light green with numerous light-brown spots	7
<i>yaoshanensis</i>	cream with small spots	orange-red without spots	12
<i>yinggelingensis</i>	immaculate cream	orange-red without spots	4, 5
<i>zhoukaiyae</i>	cream bellow with small brow spots	yellowish with grayish blotching	11

Sources: 1= Ohler et al. (2000); 2= Orlov et al. (2001); 3= Rao et al. (2006); 4= Chou et al. (2007); 5= Fei et al. (2010); 6= Zhang et al. (2011); 7= Li et al. (2012); 8= Jiang et al. (2019); 9= Mo et al. (2016); 10= Liu et al. (2017); 11= Pan et al. (2017); 12= Chen et al. (2018); 13= Ohler & Deuti (2018); 14= Yu et al. (2019); 15= Nguyen et al. (2020); 16= Ninh et al. (2020); 17= Liu et al. (2020); 18= our data

Supplementary Table S6. Morphological comparisons of *Zhangixalus lishuiensis* (Liu, Wang & Jiang) with *Zhangixalus Zhoukaiyae* (Pan, Zhang & Zhang).

Species Sex	<i>Zhangixalus lishuiensis</i>			<i>Zhangixalus Zhoukaiyae</i>			
	Males (n=3)		Female (n=1)	Males (n=6)		Females (n=3)	
	Min-Max	Mean ±SD		Min-Max	Mean ±SD	Min-Max	Mean ±SD
SVL	34.20-35.80	35.80±0.92	45.9	27.9-37.12	33.96±3.40	42.12-44.67	43.49±1.28
HL	14.90-15.80	15.27±0.47	19.2	9.49-12.66	11.47±1.16	14.19-14.65	14.46±0.24
HW	13.90-14.70	14.17±0.46	17.6	11.56-14.44	13.38±1.06	14.80-17.94	16.34±1.57
SL	5.70-6.10	5.90±0.20	7.5	3.80-5.67	5.00±0.66	5.60-5.83	5.74±0.12
ED	4.10-4.50	4.37±0.23	5.6	3.26-4.77	4.20±0.53	4.58-5.25	5.01±0.37
TD	2.30-3.20	2.60±0.52	2.6	2.16-2.54	2.34±0.17	2.73-3.12	2.91±0.20
TL	14.70-15.70	15.2±0.05	18.6	12.43-16.66	15.01±1.41	18.97-20.26	19.65±0.65
HL/SVL	0.42-0.44	0.43±0.01	0.42	0.31-0.37	0.34±0.02	0.32-0.35	0.33±0.01
HW/SVL	0.39-0.43	0.40±0.02	0.38	0.35-0.42	0.40±0.03	0.34-0.40	0.38±0.03
SL/SVL	0.16-0.17	0.17±0.00	0.16	0.13-0.17	0.15±0.01	0.13-0.14	0.13±0.01
ED/SVL	0.12-0.13	0.12±0.00	0.12	0.11-0.15	0.12±0.01	0.10-0.12	0.12±0.01
TD/SVL	0.06-0.09	0.07±0.01	0.06	0.06-0.08	0.07±0.01	0.06-0.07	0.07±0.00
TL/SVL	0.41-0.46	0.43±0.02	0.41	0.40-0.48	0.44±0.03	0.43-0.47	0.45±0.02
Color of iris	yellowish-gold			yellowish-gold			
Finger webbing	reduced			reduced			
Coloration of dorsum	immaculate pure green			immaculate green			
Coloration of belly	anteriorly white, posteriorly yellow without spots			immaculate pure pale-yellow			
Colorations of flanks	cream without blotches			cream bellow with small brow spots			
Colorations of thighs	gray without blotches			yellowish with grayish blotching			
Source	Liu et al. (2017)			Pan et al. (2017)			

Supplementary Table S7. Morphological comparisons of *Zhangixalus yaoshanensis* (Liu & Hu) and *Zhangixalus pinglongensis* (Mo, Chen, Liao & Zhou).

Species Sex	<i>Zhangixalus yaoshanensis</i>			<i>Zhangixalus pinglongensis</i>	
	Males (n=12)		Females (n=2)	Males (n=13)	
	Min-Max	Mean±SD	Min-Max	Min-Max	Mean±SD
SVL	31.6-36.4	33.9±1.3	49.2-51.1	32.0-38.5	35.9±2.3
HL	10.1-12.2	11.2±0	14.7-14.9	12.3-15.2	13.8±1.1
HW	12.4-14.8	13.5±0.7	18.5-18.7	12.7-15.7	14.5±1.1
SL	5.5-6.2	5.9±0.2	8.1-8.2	5.5-7.2	6.3±0.6
UEW	4.4-5.3	4.8±0.2	6.1-6.7	3.3-4.7	3.9±0.4
IOD	4.0-4.8	4.5±0.3	5.9-6.0	4.4-5.5	5.0±0.4
ED	4.1-4.9	4.5±0.2	5.2-6.2	4.3-5.5	4.8±0.3
TD	2.0-2.5	2.3±0.2	3.4-3.6	2.2-3.1	2.6±0.3
TL	13.4-15.8	14.9±0.6	21.1-21.3	15.3-18.1	16.3±0.9
Color of iris	grayish-gold			silvery	
Finger webbing	reduced			reduced	
Coloration of dorsum	immaculate green			immaculate green	
Coloration of belly	immaculate cream			immaculate white	
Colorations of flanks	cream with small spots			black blotches with white spots	
Colorations of thighs	orange-red without spots			black blotches with white spots and faint orange tint	
Source	Chen et al. (2018)			Mo et al. (2016)	

Supplementary Table S8. Basic call parameters of *Zhangixalus melanoleucus* **sp. nov.** as compared to other members of the genus *Zhangixalus*.

Species	Number of pulses per note	Dominant Frequency (Hz)	Sources
<i>Z. melanoleucus</i> sp. nov.	2–3 (2.25 ± 0.38)	3140 ± 47.06	<i>this work</i>
<i>Z. chenfui</i>	2–6	2348.8 ± 53.6	Matsui & Wu (1994)
<i>Z. dennysi</i>	3–5 (3.5 ± 0.6)	1360.6 ± 77.9	Wang et al. (2012)
<i>Z. dugritei</i>	10 or more	1675.0 ± 41.8	Matsui & Wu (1994)
<i>Z. jodiae</i>	6	2000	Nguyen et al.(2020)
<i>Z. omeimontis</i>	2–5	977.1 ± 49.8	Matsui & Wu (1994)
<i>Z. zhokaiyae</i>	10 or more (19.95 ± 4.7)	1510.3 ± 60.9	Fang et al. (2019)